Evidence of triple collision dynamics in partial photo-ionisation cross sections of helium

Gregor Tanner

School of Mathematical Sciences, University of Nottingham, University Park, Nottingham NG7 2RD, UK.

Nark Nyul Choi, Min-Ho Lee

School of Natural Science, Kumoh National Institute of Technology, Kumi, Kyungbook 730-701, Korea.

Achim Czasch, Reinhard Dörner

Institut für Kernphysik, Goethe-University Frankfurt, Max-von-Laue-Str. 1 60438 Frankfurt, Germany

Abstract. Experimental results on *partial* photo-ionisation cross sections of helium are analysed in the light of recent advances in the semiclassical theory of two-electron atoms. Byun *et al* [1] predict that the *total* photo-ionisation cross section below the double-ionisation threshold can, semiclassically, be described in terms of contributions associated with classical orbits starting and ending in the triple collision. The necessary modifications of the semiclassical theory for partial cross sections is developed here. It is argued that partial cross sections are also dominated by the triple collision dynamics. The expected semiclassical contributions can be identified in the Fourier transformation of the experimental data. This clearly demonstrates for the first time the validity of the basic assumptions made in [1]. Our findings explain furthermore in a natural way the self-similar structures observed in cross section signals for different channel numbers.

PACS numbers: 32.80.Fb,03.65.Sq,05.45.Mt,05.45.-a

The rich resonance spectrum of two-electron atoms below the double ionisation threshold has been explored both experimentally and numerically up to principle quantum numbers $N \approx 13 - 17$ of the remaining one-electron atom after ionisation [2, 3, 4, 5, 6, 7, 8, 9, 10]. Progress towards even higher N values thus moving closer to the three-particle break-up threshold $E = 0$ are hampered experimentally by the limited photon energy resolution and numerically by the high-dimensionality of the system. The complexity of the classical dynamics and the large number of degrees of freedom of the system have so far also restricted semiclassical calculations of individual resonances to subsets of the full spectrum and again small N values [11, 12]. Until recently it was thought that similar restrictions also apply to a semiclassical treatment of total and partial photo-ionisation cross sections for $E < 0$. The resonance density increases dramatically for energies approaching the double-ionisation threshold and individual resonances overlap and interfere leading to a strongly fluctuating cross section signal which decreases in amplitude towards the threshold [4, 5, 6]. The strong interaction between resonance poles can be regarded as a signature of the underlying chaotic classical dynamics which is also reflected in the resonance spacing distribution which shows a gradual transition towards that of random matrix theory approaching the double ionisation threshold from below [2, 6, 10].

We will consider in the following partial photo-ionisation cross sections of two-electron atoms in the asymptotic regime $E \to 0_-$. Near the threshold, electron-electron correlation effects dominate which can be observed directly in scaling laws such as Wannier's celebrated threshold law for double ionisation [13, 14] or in slow electron ionisation experiments taken across the threshold [15]; a cusp-like structure in this "zero-kinetic energy" ionisation cross section is observed which has been interpreted in terms of classical escape along the Wannier ridge leading again to a threshold law with Wannier's exponent both below and above $E = 0$ [16]. Zero-kinetic energy spectroscopy below the double ionisation threshold does, however, not resolve the complex resonance structure of the three-particle compound and the experimental signal contains thus little information about the mostly chaotic scattering dynamics of the underlying classical three-body Coulomb system.

Semiclassically, total photo-ionisation cross sections can be described in terms of closed orbit theory (COT). The theory was developed for systems such as hydrogen in external fields [17, 18] or in the context of quantum defect theory for many electron atoms [19, 20, 21] for which the dynamics near the origin is regular. Recently, the necessary modifications for a closed orbit treatment of the total photo-ionisation cross section for two-electron atoms have been presented in [1]. Starting point of a COT is the total cross section in dipole approximation written in the form

$$\sigma(E) = -4\pi\,\alpha\,\hbar\omega\,\Im\langle D\phi_i|G(E)|D\phi_i\rangle \tag{1}$$

where ϕ_i is the wave function of the initial bound state, $D = \boldsymbol{\pi}\cdot\mathbf{r}$ is the dipole operator, $\boldsymbol{\pi}$ is the polarisation of the incoming photon with angular frequency ω, and $G(E)$ is the Green function of the system at energy $E = E_i + \hbar\omega$; furthermore $\alpha = e^2/\hbar c$ is the fine-structure constant. In the semiclassical limit, the support of the wave function ϕ_i shrinks to zero relative to the size of the system reducing the integration in (1) to an evaluation of the Green function at the origin in the limit $E \to 0_-$. Writing the Green function in semiclassical approximation [17, 18, 22] thus leads to a summation over contributions from classical trajectories starting and ending at the origin.

For two-electron atoms, the origin $\mathbf{r} = (\mathbf{r}_1, \mathbf{r}_2) = \mathbf{0}$ represents the point where both electrons reach the nucleus simultaneously, that is, all three particles collide. Note

that we work in the infinite nucleus mass approximation, that is, the position of the nucleus is fixed at the origin. The presence of such triple collisions demands a careful re-evaluation of COT in the light of the three-body dynamics near the origin. The triple-collision itself forms a non-regularisable singularity of the classical equations of motion, that is, trajectories ending in a triple collisions can not be continued through the singularity. Trajectories coming close to a triple collision become extremely sensitive to initial conditions and nearby orbits approaching the collision point can be scattered into arbitrarily large angles. The triple collision singularity is in that sense infinitely unstable. This is in contrast to binary collisions which can be regularised by a suitable space and time transformation such as described in [23] leading to a smooth phase space flow in the vicinity of the collision.

A semiclassical treatment of photo-ionisation starting from (1) needs to take into account classical trajectories beginning and ending near the three-body collision $R = 0$ where $R = (\mathbf{r}_1^2 + \mathbf{r}_2^2)^{1/2}$ is the hyper-radius; the set of closed orbits usually employed in COT, namely those emerging out of and returning exactly to the triple collision point $R = 0$, are infinitely unstable and give a vanishing contribution to semiclassical expressions. These *closed triple collision orbits* (CTCO) act, however, as guiding centres for phase space regions leaving and returning to the triple-collision region. Taking the semiclassical limit $E \to 0_-$ is equivalent to $R_0 \to 0$ in appropriately rescaled coordinates where R_0 characterises the size of the initial wave function ϕ_i. By considering these limits carefully, it has been shown in [1] that the amplitude of the fluctuations in the total photo-ionisation cross section decays with a power-law according to $\sigma_{fl} \propto |E|^{\mu}$ with predicted exponent

$$\mu = \frac{1}{4}\Re\left[\sqrt{\frac{100Z-9}{4Z-1}} + 2\sqrt{\frac{4Z-9}{4Z-1}}\right] . \tag{2}$$

with Z, the charge of the nucleus. One obtains, for example, $\mu = 1.30589...$ for helium with $Z = 2$. The exponent can be obtained as a combination of stability exponents of the triple-collision singularity and differs from Wannier's exponent which describes double ionisation processes. The Fourier components of the fluctuations can furthermore be associated directly with CTCO's. This behaviour has been confirmed by quantum calculations in collinear helium, the restricted three-body Coulomb problem where the dynamics takes place along a common axis [1].

In this letter, we analyse the experimental data on partial photo-ionisation cross sections for helium presented in [4, 5] (and shown in Fig. 1a), in the light of the theoretical predictions [1]. The experiment was conducted using synchrotron radiation with a resolution of 4 meV revealing partial cross sections up to energies 78.85 eV above the ground state and reaching ionisation channels of the order $N \approx 13$. The kinetic energy of the outgoing electron was measured which yields information on the state of the remaining He^+ - ion; for experimental details, see [4]. Ref. [5] notes in particular, that the cross sections σ_N for different channels show similar patterns up to an overall shift in energy, see for example the data for $N = 4$ and $N = 5$ in the region $E < -0.02$ au in Fig. 1a; (in Fig. 1 and throughout the paper, atomic units (au) are employed). The phenomenon could be reproduced in R-matrix calculations published in the same article. In Fig. 1b, the fluctuating part of the experimental partial cross sections are shown after subtracting numerically a smooth background contribution.

In the following, we will argue semiclassically that CTCOs also dominate the fluctuations in partial ionisation cross-sections and show that collision orbits can actually be detected in the experimental data. This leads naturally to a semiclassical

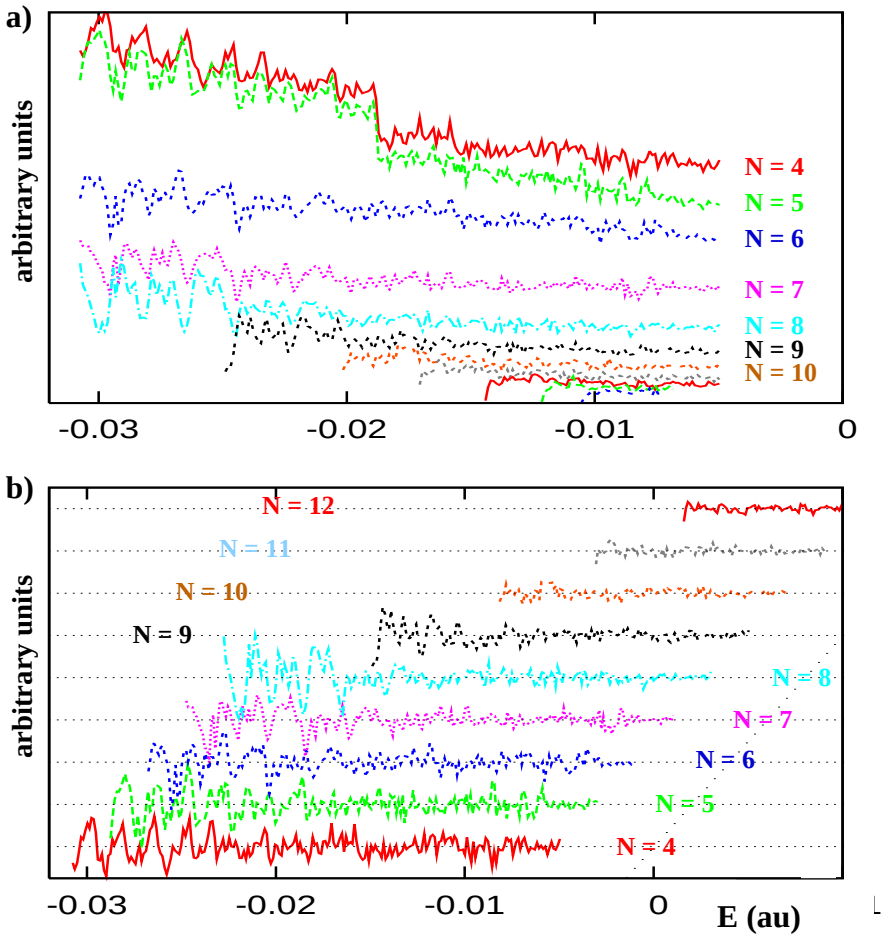

Figure 1. a) Partial cross sections as measured in [4, 5]; (the jump in the signal for $N = 4, 5$ at $E \approx -0.02$ au is due to experimental reasons; the signal for $N = 4$ was in addition shifted down towards $N = 5$). b) The fluctuating part of the cross sections for different channel numbers obtained from a) after subtracting a smooth background contribution.

explanation for the similarities seen in the cross-sections σ_N for different N. The experimentally observed slight shifts in energy between the patterns in different partial cross sections can then be explained in terms of phase differences between direct and indirect contributions as discussed in more detail later. The experimental data clearly show a decrease in the amplitude of the fluctuations as $E \to 0_-$; the exponents characterising the mean power-law decay of the fluctuations can at present not be extracted from the data with sufficient accuracy to allow a comparison with theoretical predictions; they will thus not be considered here. A detailed theory of threshold laws for partial cross sections will be presented elsewhere [24].

We start by expressing the partial cross sections σ_N in terms of the retarded Green function $G(E)$, from which a semiclassical theory can be developed. The outgoing

solution of the inhomogeneous Schrödinger equation

$$(E - H)|\chi >= D|\phi_i > \tag{3}$$

is written as

$$|\chi >= G(E)|\Phi_i > \quad \text{with } |\Phi_i >= D|\phi_i >, \tag{4}$$

and using the notation introduced after Eq. (1). In the asymptotic limit $R \to \infty$ which corresponds for fixed $E < 0$ to either r_1 or $r_2 \to \infty$, the Schrödinger equation (3) is homogeneous and separable. One obtains asymptotically for the inhomogeneous solution $|\chi >$ in the ionisation channel $(N\lambda)$

$$< r_1 N\lambda|\chi >=< r_1 N\lambda|G(E)|\Phi_i > \propto f_N^+(r_1) \quad \text{for} \quad r_1 \to \infty \tag{5}$$

where $\lambda = \{LMl_1l_2\}$ denotes the quantum numbers describing angular momenta and N is the principal quantum number of the remaining ion; furthermore, $f_N^+(r_1)$ is the outgoing Coulomb function

$$f_N^+(r_1) = \exp[i(k_N r_1 + \frac{Z-1}{k_N} \ln r_1)] \tag{6}$$

with $k_N = \sqrt{2(E - E_N)}$, the momentum of the outgoing electron. After writing the cross section as flux through the surface $R = const$, taking the limit $R \to \infty$, and using the asymptotic form of the inhomogeneous solution (4) as given in (5), we express the partial cross section σ_N in the form [25]

$$\sigma_N = \sum_\lambda \sigma_{N\lambda} = \sum_\lambda 2\pi\alpha\omega k_N \lim_{r_1\to\infty} |G(r_1 N\lambda; E)|^2 \tag{7}$$

where $G(r_1 N\lambda; E) =< r_1 N\lambda|G(E)|\Phi_i >$ and σ_N becomes independent of r_1.

The matrix elements $G(r_1 N\lambda; E)$ of the Green function can in semiclassical approximation be described in terms of classical trajectories starting at $R \le R_0$ near the origin and reaching $r_1 \to \infty$ with fixed energy E_N of the hydrogen like atom and fixed quantum numbers λ, thus determining the kinetic energy $\epsilon_N = k_N^2/2$ of the escaping electron. For details see [24]; a similar treatment applied to transport in quantum wires with fixed channel numbers can be found in [26]. We will distinguish direct escape leading from the initial region $R < R_0$ directly to ionisation and indirect contributions from trajectories entering into a predominately chaotic phase space region before ionisation, that is,

$$G(r_1 N\lambda; E) = G_{dir}(r_1 N\lambda; E) + G_{ind}(r_1 N\lambda; E). \tag{8}$$

The cross section $\sigma_{N\lambda}$ can now be written in terms of a smooth background part and a fluctuating contribution according to $\sigma_{N\lambda} = \sigma^0_{N\lambda} + \sigma^{(fl)}_{N\lambda}$ where

$$\sigma^0_{N\lambda} = 2\pi\alpha\omega k_N |G_{dir}(r_1 N\lambda; E)|^2 \tag{9}$$

$$\sigma^{(fl)}_{N\lambda} = 4\pi\alpha\omega k_N \,\Re\left[G^*_{dir}(r_1 N\lambda; E) G_{indir}(r_1 N\lambda; E)\right]. \tag{10}$$

In (10), the term $|G_{indir}|^2$ is neglected as it contains contributions from pairs of indirect trajectories which give rise to lower order corrections in the asymptotic limit $|E/E_N| << 1$.

We turn now to a brief discussion of the classical dynamics in two-electron atoms. By introducing the scaling transformation [23]

$$\mathbf{r} = \tilde{\mathbf{r}}/|E|; \quad \mathbf{p} = \sqrt{|E|}\tilde{\mathbf{p}}; \quad S = \tilde{S}/\sqrt{|E|}, \quad \mathbf{L} = \tilde{\mathbf{L}}/\sqrt{|E|}, \tag{11}$$

one studies the dynamics at fixed energy $E = -1$ where $\tilde{\mathbf{r}}, \tilde{\mathbf{p}}$ denote the scaled coordinates and momentum and $\tilde{\mathbf{L}}$ is the total scaled angular momentum. The region $R \leq R_0$ containing the initial state ϕ_i shrinks according to $\tilde{R}_0 = |E|R_0 \to 0$ for $E \to 0_-$, that is, the initial conditions approach the triple collision. Likewise, the kinetic energy of the outgoing electron diverges according to $\tilde{\epsilon}_N = \epsilon_N/|E|$ for fixed N. Expressing the angular momentum in scaled coordinates, we have $\tilde{\mathbf{L}} \to 0$ as $E \to 0$ for fixed $\mathbf{L}$; the classical dynamics takes place closer and closer to the zero angular momentum manifold. It can therefore asymptotically be characterised by trajectories in the invariant subpace $\tilde{\mathbf{L}} = 0$ which has only three degrees of freedom [12]. The part of the dynamics contributing to the semiclassical Green function $G = G_{dir} + G_{ind}$ is in scaled coordinates formed by trajectories starting closer and closer to the triple collision $R = 0$ as $|E| \propto \tilde{R}_0 \to 0$. The triple collision singularity $R = 0$ itself has a non-trivial structure and is equivalent to the phase space dynamics at $E = 0$. We will here describe only those features of the dynamics near $R = 0$ which are important for understanding the semiclassical approximations; for more details see [12, 27, 28]. Most initial conditions near the triple collision will give rise to trajectories leading to immediate ionisation of one electron. Direct orbits escaping with kinetic energy ϵ_N will contribute to the direct escape term G_{dir}; an example of such a trajectory (dashed line) is shown in Fig. 2a. Only a fraction of the phase space near $R = 0$ can enter a chaotic scattering region; these orbits all move out along the so-called Wannier orbit (WO), the trajectory of collinear and symmetric electron dynamics with $r_1 = r_2$. An example of such a indirect orbit is shown in Fig. 2a (thick full line). Likewise, trajectories inside the chaotic phase space can only leave this region after approaching the triple collision along the WO. Escaping from the triple-collision region towards ionisation with asymptotic kinetic energy $\tilde{\epsilon}_N = \epsilon_N/|E| \to \infty$ as $E \to 0_-$ can be achieved only by coming closer and closer to the triple collision. The point of closest approach, $\tilde{R}_N$, of trajectories escaping with kinetic energy $\tilde{\epsilon}_N$ vanishes for fixed N like $\tilde{R}_N \propto |E|$. The indirect part of the Green function $G_{ind}(N)$ is thus semiclassically described in terms of orbits starting and ending (in scaled coordinates) closer and closer to the triple collision before escaping with kinetic energy $\tilde{\epsilon}_N$. These trajectories approach a proper CTCO asymptotically. The phase space regions contributing to the partial Green function $G_{indir}(N)$ can thus be characterised in terms of CTCO's in the same way as the total cross section [1]. Triple collision orbits only occur in the so-called eZe space [12], a collinear subspace of the full three body dynamics where the two electrons are on opposite sides of the nucleus [23]. As $\tilde{R}_0, \tilde{R}_N \to 0$, only orbits coming close to the eZe space can start and return to the triple collision and they will do so in the vicinity of a CTCO. The dynamics in the eZe space is relatively simple as it is conjectured to be fully chaotic with a complete binary symbolic dynamics. The symbolic coding of a trajectory is here defined as:

$-$: electron 1 collides with the nucleus - $r_1 = 0$;
$+$: electron 2 collides with the nucleus - $r_2 = 0$;
c : triple - collision.

The completeness of the symbolic dynamics implies that there is exactly one CTCO for every finite binary symbols string; the shortest is the WO with code *cc*. In Fig. 2b, some short CTCOs are shown; note that orbits whose symbol code is related by the operation $+ \leftrightarrow -$ are mapped onto each other by the particle exchange symmetry $r_1 \leftrightarrow r_2$ and are thus equivalent.

CTCOs have been shown to be important for the total cross section [1] giving

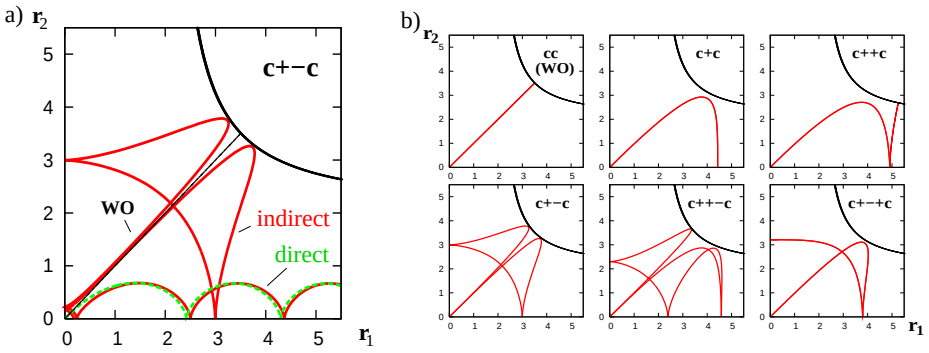

Figure 2. Triple collision dynamics and closed triple collision orbits: a) trajectories starting near the triple collision point $r_1 = r_2 = 0$ and leading to ionisation with fixed energy of the escaping electron; dashed (green) line: direct path; thick full (red) line: indirect path, here close to the CTCO $c+-c$; b) some short CTCOs together with binary symbol code.

the main contributions in a modified semiclassical closed orbit treatment of photo-ionisation. The fact that CTCOs also enter partial cross section here is due to the above-mentioned escape mechanism which is special to two-electron atoms. Swarms of indirect trajectories starting at $R = R_0$, following a similar path in the chaotic region and then escaping with fixed kinetic energy ϵ_N can for $E \to 0$ be linked to a single CTCO together with a direct-escape orbit. Likewise, the phase space region leading from $R < R_0$ to direct escape can be represented by a single trajectory. We thus write

$$G_{dir} \approx A_0(N\lambda) e^{iS_0(r_1 N\lambda;E) - i\nu_0(r_1 N\lambda;E)\pi/2}\,; \tag{12}$$

$$G_{ind} \approx e^{iS_0(r_1 N\lambda;E) - i\nu_0(r_1 N\lambda;E)\pi/2} \times \sum_{\mathrm{CTCO}} A_j(N\lambda;E) e^{iS_j(E) - i\nu_j\pi/2}. \tag{13}$$

Here S_0, ν_0 are the action and Maslov index along the direct orbit, respectively, and S_j, ν_j are those along a CTCO starting from and ending in the triple collision. ‡ The initial wave function Φ_i and the dynamics in phase space leading to direct orbits is not sensitive to the threshold energy $E = 0$. The pre-factor A_0 will thus pick up a smooth energy dependence and can be treated as constant at the threshold. The singular behaviour of the classical dynamics near the triple collision for CTCO contributions leads to a universal scaling behaviour of the terms A_j as $E \to 0_-$ as described in [1]; the semiclassical analysis suggests the same scaling law as for the total cross section, that is,

$$A_j(N\lambda;E) = a_j(N\lambda)\,|E|^{\mu} \tag{14}$$

for $E \to 0_-$ and fixed N with exponent given by Eq. (2). From (7), (10), (12), (13) and (14), we obtain an approximation to the fluctuating part of the partial cross sections

‡ We note that extra phase contributions arise due to the stationary phase approximation leading to the fixed kinetic energy condition in the outgoing channel; these phases are not energy dependent and are here absorbed in the pre-factors.

in the form

$$\sigma_N^{(fl)} \approx 4\pi\alpha\omega k_N |E|^\mu \, \Re \left(\sum_{\mathrm{CTCO}} \mathcal{A}_j(N) e^{iz\tilde{S}_j - i\nu_j \pi/2} \right) \tag{15}$$

where the pre-factor $\mathcal{A}_j(N)$ are of the form $\mathcal{A}_j(N) = \sum_\lambda a_j(N\lambda) A_0(N\lambda)$ and $z = 1/\hbar\sqrt{|E|}$; note, that the $\mathcal{A}_j(N)$ are in general complex valued and will add extra (energy independent) phases.

The semiclassical treatment above suggests that a Fourier transformation of $\sigma_N^{(fl)}$ in terms of the variable z would reveal peaks at the actions of classical CTCOs. Such an analysis has been carried out using the experimental data from [4, 5] setting the origin of the energy scale at the double ionisation threshold, that is, 79.014 eV above the ground state of helium. After subtracting a smooth background by fitting a low-order polynomial to the experimental data, the fluctuating signal as shown in Fig. 1b is transformed using the Lomb - algorithm [29], a Fourier transform technique particularly useful for unevenly spaced data sets. (Note that the experimental data are taken at uniform steps in E which leads to an increasing step-size in z.) The peak heights in the experimental partial cross sections are roughly of the same size for fixed energy independent of N. The corresponding Fourier signals thus show structures of similar size, see inset in Fig. 3; to enhance the resolution, we averaged over the transformed cross sections for $N = 4 - 8$ for which data sets in energy intervals of the same length are available. The resulting averaged Fourier signal is shown in Fig. 3 together with the values of the actions of short CTCOs such as depicted in Fig. 2b.

Despite the fact that the energy range available is rather limited, there are clear correlations between the positions of the pronounced peaks and the actions of CTCOs; (note, that the high-resolution Fourier signal presented in [1] for the total cross section was obtained using a much larger energy range - up to $N = 50$ - in the collinear eZe model). The Fourier signal shown in Fig. 3 is a clear indication that photo-ionisation cross sections of three dimensional helium are indeed dominated by the triple collision dynamics in the collinear eZe subspace. The similarities in the partial cross sections noted in [5], are now naturally explained in terms of the semiclassical expansion (15); the dominant terms contribute asymptotically with the same phase - the actions of CTCOs - which will produce similar modulations in the overall signal for different N. The slight energy shifts observed in the cross section pattern when comparing signals for nearby N values as can be seen Fig. 1 are caused by energy independent phases in the $A_j(N)$'s entering Eq. (15); a detailed analysis will be presented in [24].

Due to the degeneracy of the $c + c$ and $c - c$ orbits related by particle exchange symmetry, the peak associated with the code + is about twice as high as the WO - peak. A similar phenomena was observed for the total cross section in [1]. Otherwise, the semiclassical amplitudes decrease in general exponentially with the length of the symbol code which can also be seen in the Fourier data. Furthermore, a peak at an action smaller than that of the shortest CTCO, the WO with action $\tilde{S}/2\pi = 3.5$, can be observed in Fig. 3. We note, that the peak is at $\tilde{S}/2\pi = \sqrt{2}$, which is the action of the asymptotic threshold orbit where the outer electron escapes with zero kinetic energy leaving the inner electron at a total energy $\tilde{E}_N = -1$. The peak may thus stem from non-perfect cancellations between actions for direct and indirect contributions especially near the channel thresholds. It is a feature special to partial cross sections and is not expected to be observed in total photo-ionisation signals.

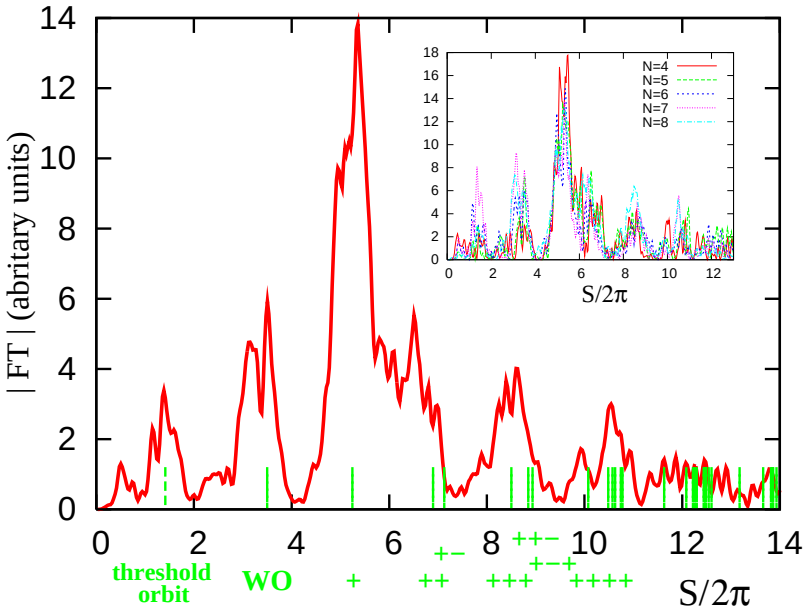

Figure 3. The Fourier spectrum of the fluctuating part of the partial cross section in Fig. 1 averaged over $N = 4-8$; the actions of CTCOs are marked on the axis together with their respective binary symbol code. Inset: individual Fourier signals.

In conclusion, we show that the fluctuations in the partial photo-ionisation cross section in helium below the double ionisation threshold are semiclassically dominated by contributions from closed triple collision orbits. This explains naturally the similarities observed in different partial cross sections and is a clear evidence that both partial and total cross sections are dominated by the low-dimensional collinear eZe dynamics [1]. It is at present not possible to extract threshold laws such as stated in Eq. (14) from the data; a detailed account of the theory including the N-dependence of the amplitude terms due to the direct and indirect contributions will be presented elsewhere [24].

Acknowledgments

Nark Nyul Choi acknowledges financial supports by the Kumoh National Institute of Technology for the project 2006-104-067 and the Royal Society for visiting the University of Nottingham where parts of this work were carried out.

Bibliography

[1] C. W. Byun, N. N. Choi, M.-H. Lee and G. Tanner, *Scaling laws for the photo-ionisation cross section of two-electron atoms*, to be published in Phys. Rev. Lett. (2007); arXiv.org: physics/0701086.

[2] R. Püttner, B. Grémaud, D. Delande, M. Domke, M. Martins, A. S. Schlachter and G. Kaindl, Phys. Rev. Lett. **86**, 3747, (2001).

[3] Y. H. Jiang, R. Püttner, R. Hentges, J. Viefhaus, M. Poiguine, U. Becker, J. M. Rost and G. Kaindl, Phys. Rev. A **69**, 042706 (2004).

[4] A. Czasch *et al*, Physica Scripta **T110**, 141, (2004); A. Czasch, *Doppelt hoch angeregte Zustände von Helium*, PhD-thesis, J. W. Goethe Universität Frankfurt (2004).
[5] A. Czasch *et al*, Phys. Rev. Lett. **95**, 243003, (2005).
[6] Y. H. Jiang , *Doubly excited helium: from strong correlations to chaos*, PhD-thesis, Freie Universität Berlin (2006).
[7] D. Delande, unpuplished - see [6].
[8] A. Bürgers, D. Wintgen and J.-M. Rost, J. Phys. B **28**, 3163 (1995).
[9] H. W. van der Hart and C. H. Greene, Phys. Rev. A, **66**, 022710 (2002).
[10] A.-T. Le, T. Morishita, X.-M. Tong and C. D. Lin, Phys. Rev. A **72**, 032511 (2005).
[11] G. Tanner, K. Richter and J. M. Rost, Rev. Mod. Phys. **72**, 497 (2000).
[12] N. N. Choi M.-H. Lee and G. Tanner, Phys. Rev. Lett. **93**, 054302 (2004); M.-H. Lee, G. Tanner and N. N. Choi, Phys. Rev. E **71**, 056208 (2005).
[13] G. H. Wannier, Phys. Rev. **90**, 817 (1953).
[14] H. Kossmann, V. Schmidt and T. Anderson, Phys. Rev. Lett. **60**, 1266 (1988).
[15] S. Cvejanovic and F. H. Read, J. Phys. B **14**, 1841 (1974); S. Cvejanovic, R. C. Shiell and T. J. Reddish, J. Phys. B **28**, L707 (1995); D. B. Thompson, P. Bolognesi, M. Coreno, R. Camilloni, L. Avaldi, K. C. Prince, M. de Simone, J. Karvonen and G. C. King, J. Phys. B **31**, 2225 (1998).
[16] U. Fano, J. Phys. B **14**, L401 (1974); F. H. Read, J. Phys. B **17**, 3965 (1984); F. H. Read and S. Cvejanovic, J. Phys. B **21**, L371 (1988).
[17] E. B. Bogomolny, Sov. Phys. JETP **69**, 275 (1988).
[18] M. L. Du and J. B. Delos, Phys. Rev. A **38**, 1896 and 1913 (1988).
[19] D. Delande, K. T. Taylor, M. H. Halley, T. van der Veldt, W. Vassen and W. Hogervorst, J. Phys. B **27** 2771 (1994).
[20] P. A. Dando, T. S. Monteiro, D. Delande and K. T. Taylor, Phys. Rev. Lett. **74**, 1099 (1995); B. Hüpper, J. Main and G. Wunner, Phys. Rev. Lett. **74**, 2650 (1995).
[21] B. E. Granger and C. H. Greene, Phys. Rev. A **62**, 012511 (2000); T. Bartsch, J. Main and G. Wunner, Phys. Rev. A **67**, 063411 (2003).
[22] M. C. Gutzwiller, *Chaos in Classical and Quantum Mechanics* (Springer, New York, 1990).
[23] K. Richter G. Tanner and D. Wintgen, Phys. Rev. A **48**, 4182 (1993).
[24] N. N. Choi, M.-H. Lee and G. Tanner, in preparation (2007).
[25] H. Friedrich, *Theoretical Atomic Physics, 3rd Ed* (Springer-Verlag Berlin Heidelberg 2005).
[26] R. A. Jalabert, H. U. Baranger and A. D. Stone, Phys. Rev. Lett. **65**, 2442 (1990).
[27] M.-H. Lee, N. N. Choi and G. Tanner Phys. Rev. E **72**, 066215 (2005).
[28] Z.-Q. Bai, Y. Gu and J. M. Yuan, Physica D **118**, 17 (1998).
[29] W. H. Press, S. A. Teukolsky, W. T. Vetterling and B. P. Flannery, *Numerical Recipes*, (Cambridge University Press, Cambridge, 1994).